SUPPLEMENTARY MATERIAL

Nickel hexacyanoferrate/graphene thin film: a candidate to cathode in aqueous metal-ion batteries

Eduardo G.C. Neiva[1] and Aldo J.G. Zarbin[*]

Departamento de Química, Universidade Federal do Paraná (UFPR), CP 19081, CEP 81531-990, Curitiba, PR, Brazil.

---

* Corresponding author

Phone/FAX: +55-41-33613176

Email: aldozarbin@ufpr.br

[1]Present address: Department of Chemistry, University of Blumenau, Blumenau, SC, CEP 89012900 Brazil.

E-mail address: eneiva@furb.br

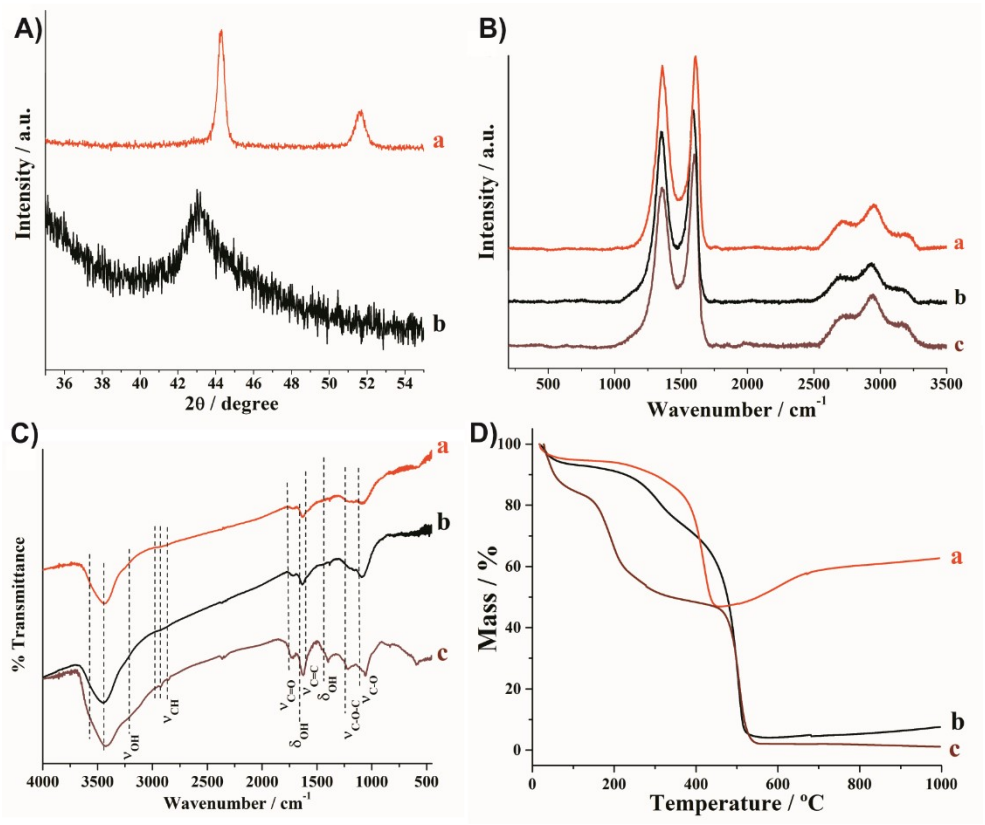

Figure S1. (A) XRD profile of (a) rGO/Ni and (b) rGO; (B) Raman spectra of (a) rGO/Ni, (b) rGO and (c) GO; (C) FT-IR spectra of (a) rGO/Ni, (b) rGO and (c) GO; (D) TGA curves of (a) rGO/Ni, (b) rGO and (c) GO.

As shown in Figure S1A, nickel ions were successful reduced to metallic nickel with face-centered cubic structure characterized by d_{111} and d_{200} equals to 2.045 (44.3°) and 1.771 Å (51.6°), respectively [1]. Using the Scherrer equation a crystallite size of 44 nm is found for rGO/Ni. A broad peak is also observed at d_{100} = 2.099 Å (43.1°) attributed to rGO [2]. These XRD patterns demonstrate the simultaneous reduction of GO and Ni^{2+} in a single step.

The Raman spectra (Figure S1B) exhibit the D (1359 cm^{-1}), G (1592 cm^{-1}), D' (1615 cm^{-1}), G' (2709 cm^{-1}), D+G (2945 cm^{-1}) and 2D' (3201 cm^{-1}) bands attributed to graphene-based materials [3]. As expected, the reduction of GO to rGO increase the D band intensity due the production of

defects in the carbonaceous structure of the graphene as carbon vacancies and Stone-Wales defects [3].

The FT-IR spectra are shown in Figure S1C and confirm the reduction of GO. It is clear to observe the decrease in the intensity of the bands attributed to the surface functional groups of GO at 3570/3425/3190 (ν_{OH}), 2962/2920/2850 (ν_{CH}), 1726 ($\nu_{C=O}$), 1625 (δ_{H-O-H}), 1574 ($\nu_{C=C}$), 1402 (δ_{C-OH}), 1220 (ν_{C-O-C}) and 1060 cm^{-1} (ν_{C-O}) [4]. However, the remaining of these bands indicate a partial reduction of GO to rGO.

The thermogravimetric curves obtained in air atmosphere (Figure S1D) corroborates the FT-IR data indicated by the decrease of the mass losses due to the GO functional groups, in the range of 120 to 400 °C, after reduction, leading to C/O rates of 1.24 and 3.52 to GO and rGO, respectively. The metallic nickel content in rGO/Ni nanocomposite is 46.9 %. The TGA curves also show a mass increase beginning at 470 °C for rGO/Ni which is related to the nickel oxidation. A summary of the main events observed in TGA curves is shown in the Table S1.

Table S1. A summary of the main events extracted from the TGA curves. The temperature range in which each event is observed is demonstrated in parenthesis

	H_2O/%	**Oxygenated groups/%**	**Oxygenated groups and/or carbon/%**	**Ni*/%**	**NiO/%**
rGO/Ni	5.3 (20-120 °C)	----	47.8 (240-460 °C)	46.9	62.6
rGO	7 (20-120 °C)	19.5 (120-400 °C)	68.6 (400-600 °C)	----	----
GO	15.9 (20-120 °C)	36.6 (210-400 °C)	45.5 (400-600 °C)	----	----

* – Ni % was estimated from NiO % extracted from TGA.

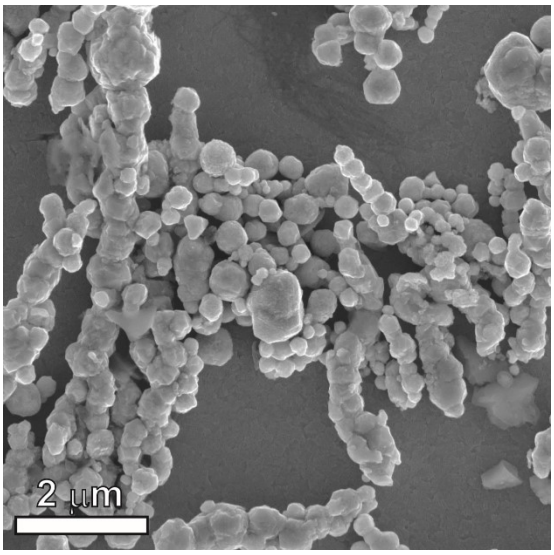

Figure S2. FEG-SEM image of Ni control sample.

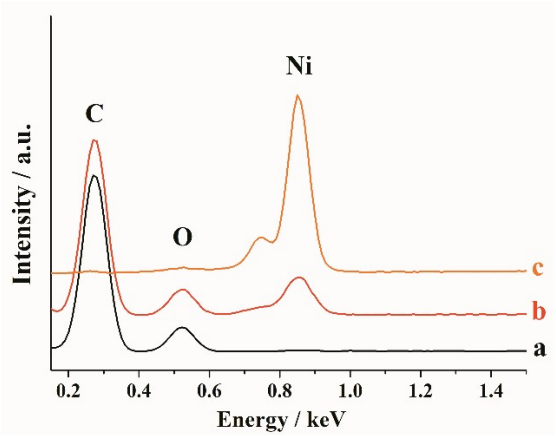

Figure S3. EDS spectra of the rGO (a), rGO/Ni nanocomposite (b) and Ni (c).

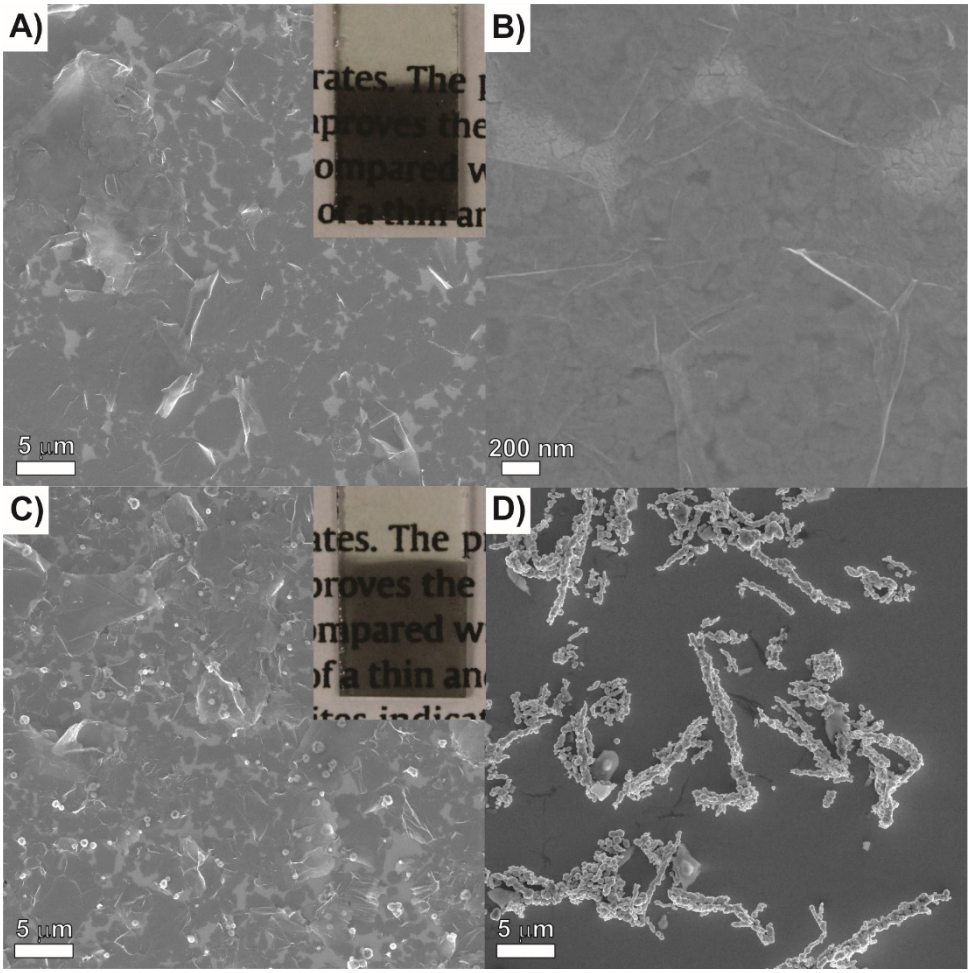

Figure S4. FEG-SEM images of rGO (A,B), rGO/Ni (C) and Ni (D) thin films over ITO electrodes. The photographic images of the thin films are shown in the insets in (A) and (C).

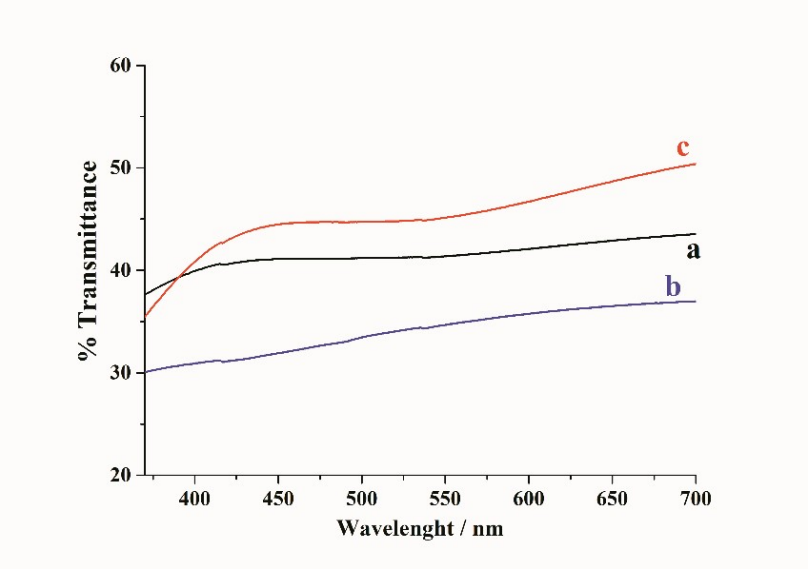

Figure S5. Transmittance spectra of the films: (a) rGO/Ni; (b) rGO; (c) rGO/NiHCFe.

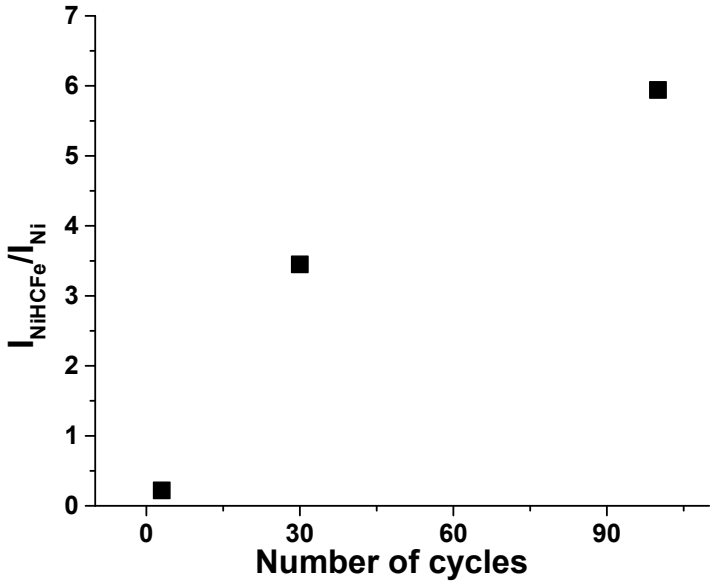

Figure S6. NiHCFe (17.5º)/Ni (44.5º) intensity peak ratio as function of cycling of rGO/Ni in 0.1 mol L^{-1} KCl, 1 mmol L^{-1} $K_3[Fe(CN)_6]$ and pH 3.

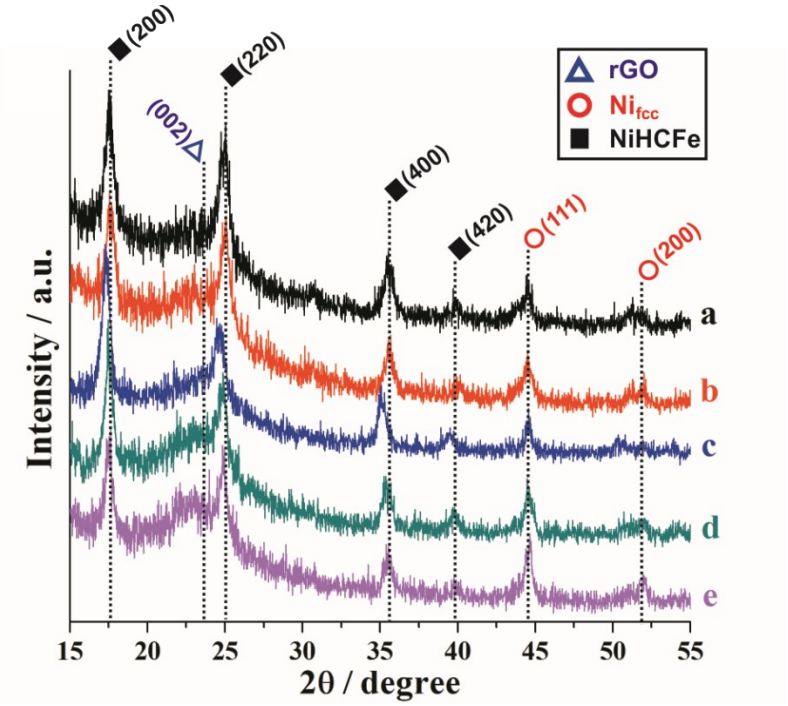

Figure S7. X-ray diffractograms of rGO/NiHCFe as prepared (a) and after 100 cycles in 0.1 mol L^{-1} KCl (b), NaCl (c) or LiCl (d). (e) X-ray diffractogram of the film re-cycled 100 times in 0.1 mol L^{-1} KCl aqueous solution after the 100 cycles cycling in LiCl.

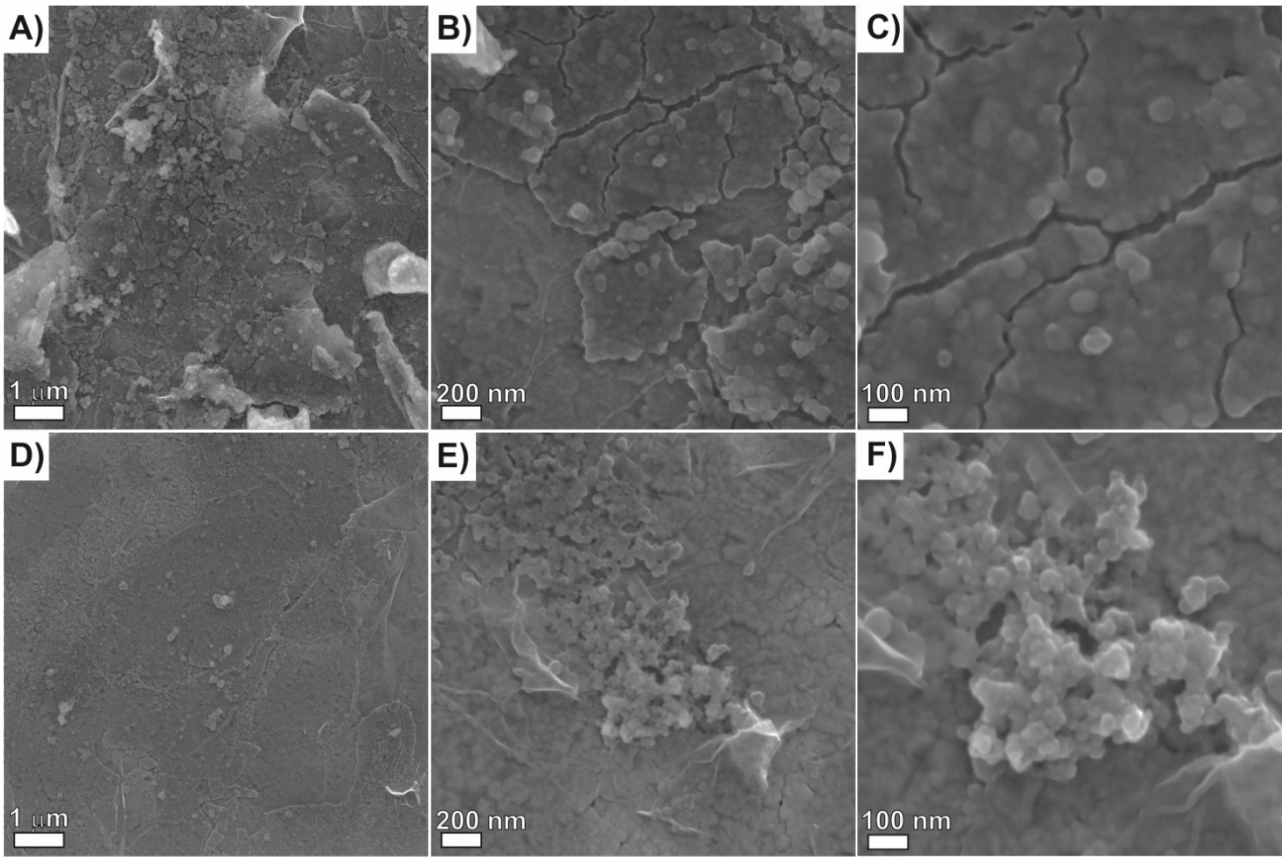

Figure S8. FEG-SEM of rGO/NiHCFe after 100 cycles in 0.1 mol L^{-1} of KCl (A-C) and LiCl (D-F).

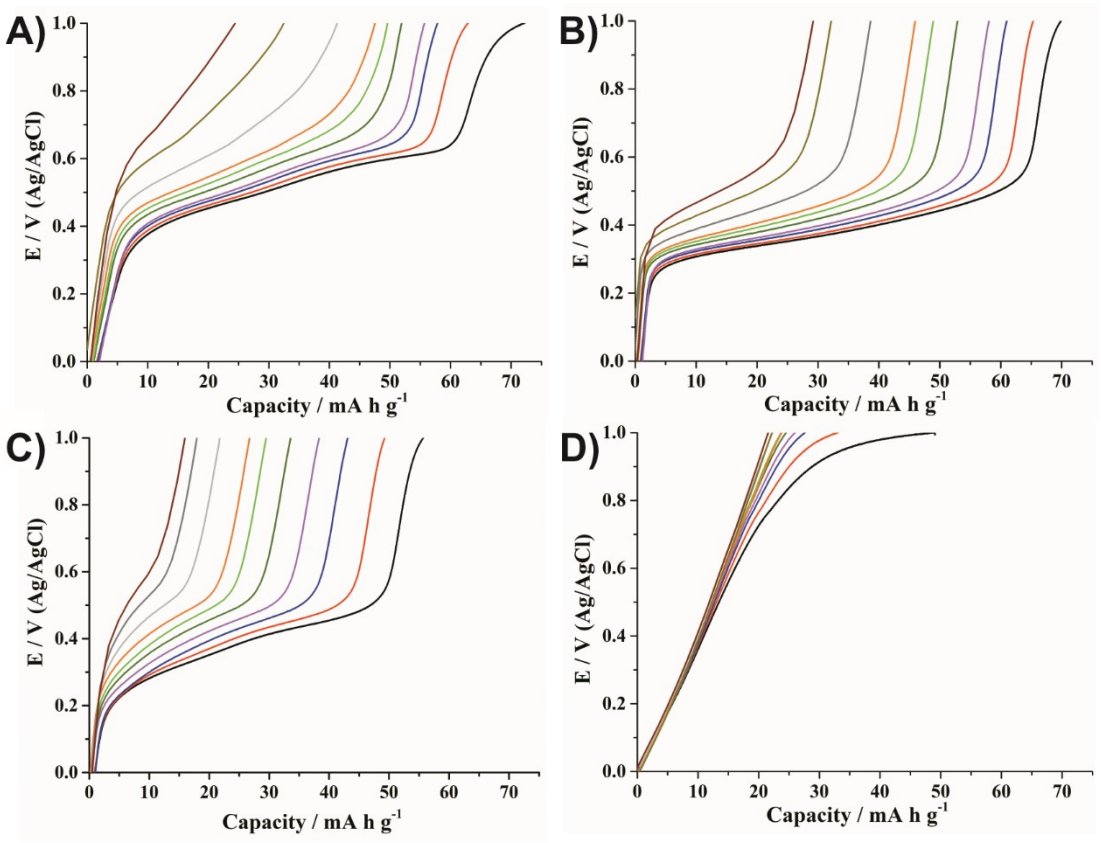

Figure S9. Charge curves of rGO/NiHCFe in 0.1 mol L^{-1} aqueous solution of KCl (A), NaCl (B) and LiCl (C); (D) Charge curves of rGO in 0.1 mol L^{-1} KCl. Data collected at CD current densities of 0.4, 0.8, 1.6, 2.4, 4, 6, 8, 16, 32 and 58.8 A g^{-1} (curves from right to left, respectively - from 0.4 A g^{-1} - black line -, to 58.8 A g^{-1} - brown line).

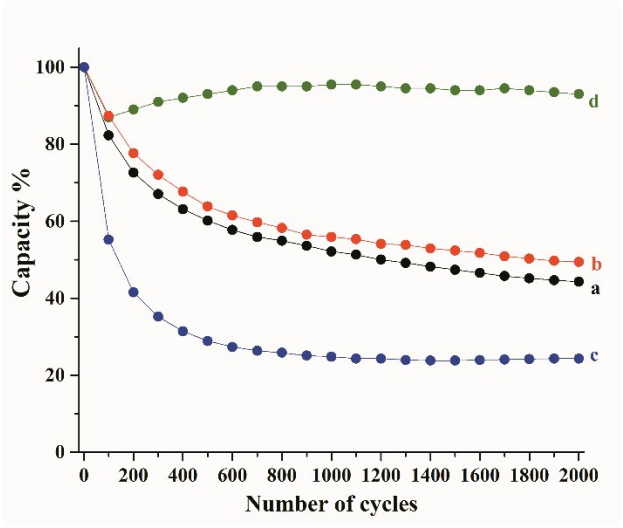

Figure S10. Relative capacity (%) as a function of CD cycles of rGO/NiHCFe film in 0.1 mol L^{-1} aqueous solution of KCl (a), NaCl (b) or LiCl (c), and for rGO film in 0.1 mol L^{-1} aqueous solution of KCl (d), at 4.1 A g^{-1}.

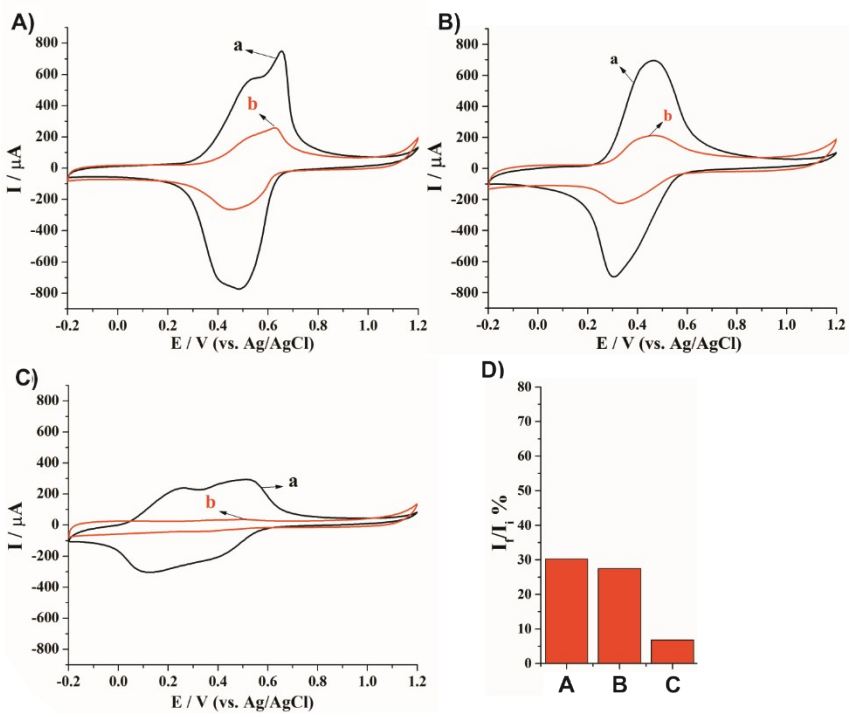

Figure S11. 10th cyclic voltammograms of rGO/NiHCFe before (a) and after (b) 2000 charge-discharge cycles in 0.1 mol L^{-1} aqueous solution of (A) KCl, (B) NaCl or (C) LiCl. (D) Anodic peak current percentage after 2000 charge-discharge cycles.

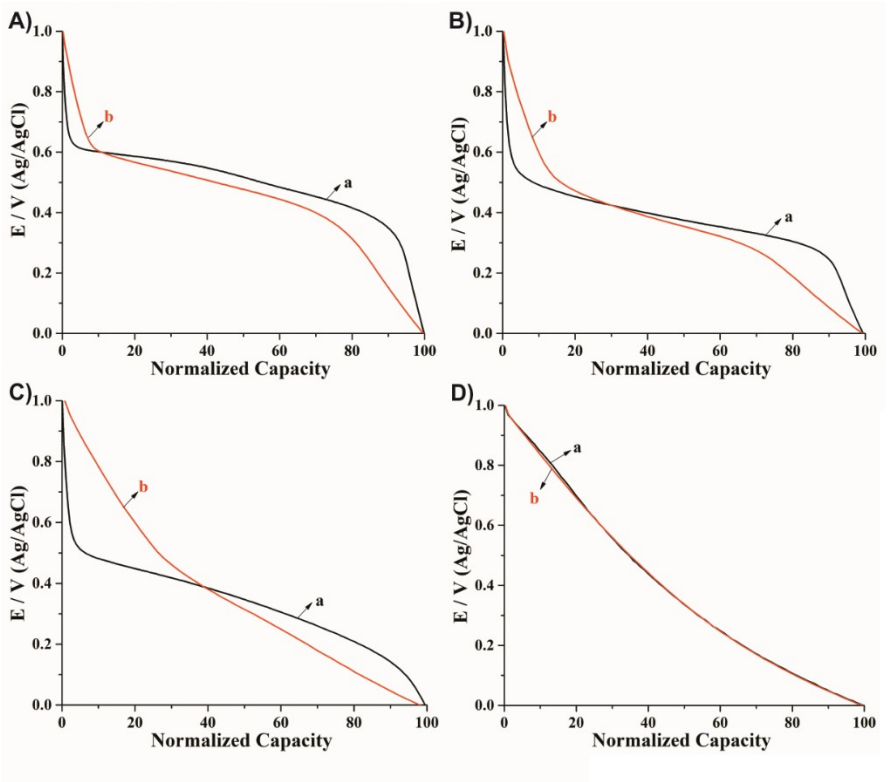

Figure S12. 1st (a) and 2000th (b) discharge cycles of rGO/NiHCFe in 0.1 mol L^{-1} aqueous solution of (A) KCl, (B) NaCl or (C) LiCl, and of rGO in aqueous solution of 0.1 mol L^{-1} KCl (D).

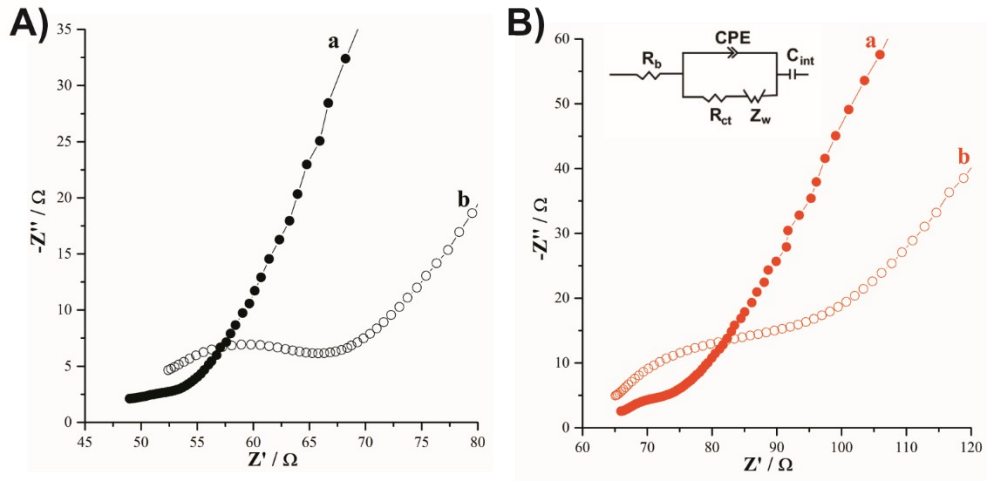

Figure S13. Electrochemical impedance spectra of rGO/NiHCFe, performed in (A) 0.1 mol L^{-1} aqueous solution of KCl and (B) 0.1 mol L^{-1} aqueous solution of NaCl before (a) and after (b) 2000 charge-discharge cycles. The inset in (B) is the equivalent circuit adopted.

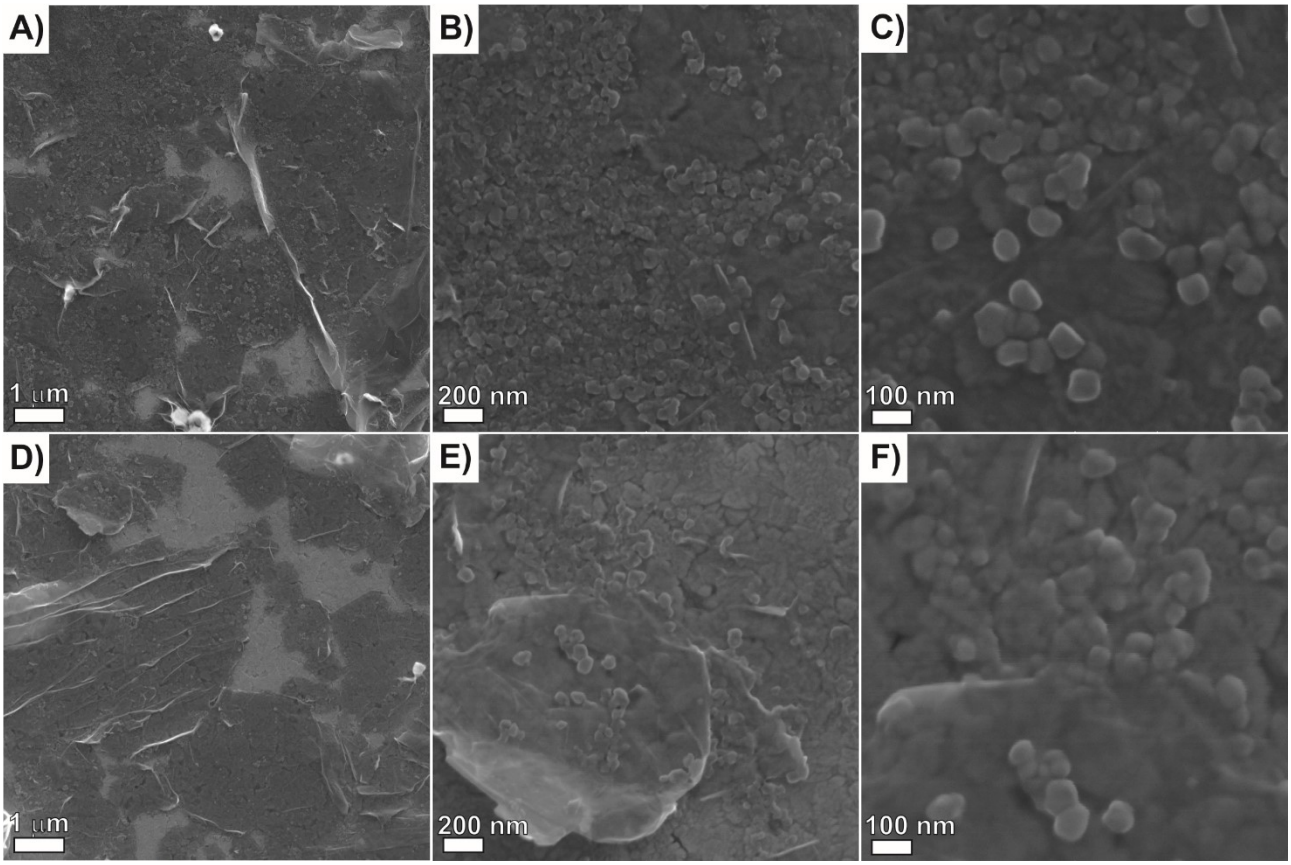

Figure S14. (A-C) FEG-SEM images of rGO/NiHCFe after 2000 charge-discharge cycles in 0.1 mol L^{-1} KCl and (D-F) LiCl.

References:

1. E. G. C. Neiva, M. F. Bergamini, M. M. Oliveira, L. H. Marcolino Jr and A. J. G. Zarbin, PVP-capped nickel nanoparticles: Synthesis, characterization and utilization as a glycerol electrosensor. Sens. Actuators B Chem., 2014, 196, 574-581.

2. L. Hostert, E. G. Neiva, A. J. Zarbin and E. S. Orth, Nanocatalysts for hydrogen production from borohydride hydrolysis: graphene-derived thin films with Ag-and Ni-based nanoparticles. J. Mater. Chem. A, 2018, 6, 22226-22233.

3. E. G. C. Neiva, M. M. Oliveira, M. F. Bergamini, L. H. Marcolino and A. J. G. Zarbin, One material, multiple functions: graphene/$Ni(OH)_2$ thin films applied in batteries, electrochromism and sensors. Sci. Rep., 2016, 6, 33806.

4. H. Mehl, C. F. Matos, E. G. C. Neiva, S. H. Domingues and A. J. G. Zarbin, Efeito da variação de parâmetros reacionais na preparação de grafeno via oxidação e redução do grafite. Quim. Nova, 2014, 37, 1639-1645.